Structure of an icosahedral Al-Mn quasicrystal

Akiji Yamamoto
National Institute for Research in Inorganic Materials, Sakura-mura, Niihari-gun, Ibaraki 305, Japan

Kenji Hiraga
Institute for Materials Research, Tohoku University, Sendai 980, Japan
(Received 25 September 1987; revised manuscript received 12 November 1987)

A structure model of an icosahedral Al-Mn quasicrystal is proposed based on the structure-factor calculation and the x-ray and neutron powder-diffraction patterns of rapidly solidified Al-Mn alloys. The model has a local atomic arrangement similar to that of the cubic α-Al-Mn-Si and has icosahedral point symmetry. To derive the model six-dimensional description of the three-dimensional Penrose lattice is extended to more general quasicrystals. The model explains the x-ray and neutron diffraction intensity, chemical composition, and density of the icosahedral quasicrystal.

I. INTRODUCTION

Since the discovery of a quasicrystal with icosahedral point symmetry in a rapidly solidified Al-Mn alloy by Shechtman *et al.*,[1] extensive studies have been made to clarify this nonperiodic structure giving a sharp diffraction pattern.[2-8] There are three methods to construct such nonperiodic quasicrystal packings: deflation-rule approach,[9-11] projection approach,[5,12] and generalized dual method.[13] Several models have been proposed on the basis of the above three methods or of the high-resolution transmission electron microscopy.[4,7,13-19] In order to determine the structure of the Al-Mn alloy, it is important to show that the model explains the diffraction intensity. Four groups have calculated the structure factors for several models. Levine and Steinhardt,[14] Duneau and Katz,[4] and Elser and Henley[7] have shown simple models giving diffraction patterns similar to the observed ones in the Al-Mn alloy. In these models only one kind of point atom is taken into account, so these are incomplete as models of an Al-Mn quasicrystal. The results, however, suggest that the structure is related to the three-dimensional (3D) Penrose lattice.[9-11] Ishihara and Shingu[17] generalized the projection method to treat more realistic cases and calculated the structure factors of two models which give reasonable chemical compositions, densities, and interatomic distances. Unfortunately, these models cannot explain the diffraction intensity of the Al-Mn alloy. For other models, the diffraction intensity has not been shown. Therefore the model which explains the diffraction intensity and gives a reasonable chemical composition has not yet been found.

Apart from the icosahedral symmetry, Elser and Henley pointed out that the α-Al-Mn-Si (α phase) gives a diffraction intensity similar to that of the quasicrystal for many reflections and this can be regarded as the cubic modification of the icosahedral quasicrystal.[7] This suggests that the icosahedral phase has similar local atomic configuration to the α phase. Guyot and Audier[20] proposed such a model, but its diffraction pattern has not been shown.

In this paper we apply the section method[8,21] to the Al-Mn alloy in order to derive the structure model of an icosahedral quasicrystal, calculate the structure factors for several models including the Guyot-Audier model, and compare the results. This method is equivalent to the projection method but it is more convenient to consider the symmetry of the quasicrystals. Similar to the superspace description of the modulated structures, the structure of the quasicrystal is given by the three-dimensional section of the crystal in the superspace and its symmetry is specified by a superspace group. In particular, the superspace group explains the systematic extinction rules due to the hyperscrew axis and hyperglide plane which are observed in the decagonal phase (d phase) of an Al-Mn quasicrystal, though no such rule exists in the icosahedral phase (i phase) treated in this paper. Therefore the section method is appropriate to treat all the quasiperiodic crystals based on a unified method. In the present icosahedral case, the structure is given in the six-dimensional (6D) space and its symmetry is specified by a six-dimensional superspace group.

The atomic configuration is derived from a six-dimensional periodic structure as a 3D section, while the diffraction pattern is regarded as the projection of the Fourier spectrum of the 6D crystal onto the 3D space. This is similar to the superspace approach in three-dimensionally modulated structures.[22-24] Since only powder-diffraction patterns are available at present for quantitative diffraction intensity and the powder data provide limited information, we use x-ray and neutron powder-diffraction data to check the validity of the model. The latter gives information independent of the former because the scattering factor is quite different from that of x ray data. In particular, when an appropriate number of Mn atoms are replaced by Fe atoms, we can get the contribution only from the Al atom, provided that Mn and Fe are randomly distributed at the same site.

The arrangement of the paper is as follows. In Sec. II, we define the 6D coordinate system and discuss the indexing problem occurring in the quasicrystal. A model is

proposed in Sec. III. Its structure factor is given in Sec. IV. In Sec. V, the calculated diffraction patterns are compared with the x-ray and neutron powder-diffraction experiments, and in the last section the other models and implications obtained from the present analysis are discussed.

II. ICOSAHEDRAL LATTICE IN THE SIX-DIMENSIONAL SPACE

A. Hypercubic and icosahedral lattices

The structure analysis is based on the 6D description of an icosahedral quasicrystal. The real 3D structure is given by a 3D section of a periodic structure in the 6D space, while the diffraction pattern is given by the projection of a 6D reciprocal lattice onto the usual 3D space as in the 6D description of modulated structures with 3D modulation.[24] In order to calculate the structure factor of a nonperiodic structure in the 3D space, a model in the 3D space is embedded into a periodic 6D crystal. Then the structure factor is given by the Fourier spectra of the 6D crystal.

The diffraction pattern and structure of an icosahedral quasicrystal are conveniently described in the 6D icosahedral coordinate system. The 6D space is divided into the 3D usual space and its orthogonal complement. We call these subspaces the external and internal spaces. When a reciprocal-lattice vector is divided into the external and internal components, the former represents the position of the diffraction spot in the real space. The diffraction pattern is indexable by using the six vectors $\mathbf{a}_i$ which are directed to the face centers of the regular dodecahedron. These have the orthogonal coordinates

$$\mathbf{a}_1=(0,0,1)\ ,$$

$$\mathbf{a}_j=(\sin\theta\cos(2\pi j/5),\sin\theta\sin(2\pi j/5),\cos\theta) \qquad (j=2,3,\ldots,6) \quad (1)$$

where θ is the angle between the nearest fivefold axes and is given by $\arccos(1/\sqrt{5})$. The vectors construct the basis of the integral matrix representation of the icosahedral point group. These are, on the other hand, regarded as the projection of the unit vectors in the 6D reciprocal lattice. From the action of the icosahedral symmetry operators to these vectors, we have the corresponding internal components: $\mathbf{a}_1$ and $-\mathbf{a}_{2j}$.[8] The unit vectors in the 6D reciprocal lattice are expressed as

$$\mathbf{d}_1^*=\frac{1}{2a}\left[\mathbf{a}_1,\frac{1}{c}\mathbf{a}_1\right],\quad \mathbf{d}_j^*=\frac{1}{2a}\left[\mathbf{a}_j,\frac{-1}{c}\mathbf{a}_{2j}\right], \qquad (2)$$

and their reciprocal vectors are

$$\mathbf{d}_1=a(\mathbf{a}_1,c\mathbf{a}_1),\quad \mathbf{d}_j=a(\mathbf{a}_j,-c\mathbf{a}_{2j})\ \ (j=2,\ldots,6)\ , \qquad (3)$$

where a is the lattice constant and c is an arbitrary real number.

The metric tensor has a form

$$\begin{bmatrix} A & B & B & B & B & B \\ B & A & B & -B & -B & B \\ B & B & A & B & -B & -B \\ B & -B & B & A & B & -B \\ B & -B & -B & B & A & B \\ B & B & -B & -B & B & A \end{bmatrix} \qquad (4)$$

where A and B are $a^2(1+c^2)$ and $a^2(1-c^2)/\sqrt{5}$. The metric tensor for the reciprocal lattice has the same form as (4), but A and B are then $(1+c^{-2})/(4a^2)$ and $(1-c^{-2})/(4\sqrt{5}a^2)$. When $c=1$, the unit vectors are mutually orthogonal and the lattice is hypercubic.

The diffraction vector is assigned with six integers $h_1,\ldots,h_6$ as $\mathbf{q}=\sum_j h_j\mathbf{d}_j^*$. When we decompose a reciprocal-lattice vector $\mathbf{q}$ into the external-space component $\mathbf{q}^e$ and the internal-space component $\mathbf{q}^i$, $\mathbf{q}^e$ represents the observed position of the reflection from the definition mentioned above while $\mathbf{q}^i$ is related to the diffraction intensity as shown in Sec. IV.

B. Bravais lattice and indexing problem

There are three Bravais lattices in the icosahedral system in the 6D space, which are denoted as the primitive, body-centered, and face-centered lattices.[8] These are distinguished by the extinction rules for general reflections. The primitive lattice has no extinction rules. For the body-centered lattice, the reflection condition is $\sum_i h_i$ even, and for the face-centered one, it is expressed as h_i $(i=1,2,\ldots,6)$ all even or all odd. Noting that the last case also fulfills the condition for the body-centered lattice, we can easily distinguish the primitive lattice from the other two: If we have the reflections with $\sum_i h_i$ odd (odd-parity reflections) then the lattice is primitive. The determination of the Bravais lattice is therefore simple. However, we have to note that the indexing of the reflection is not unique in the icosahedral quasicrystal as discussed by Elser.[5] If the odd-parity reflections do not exist, it is possible to take other unit vectors $\mathbf{d}_i'$ which are related to $\mathbf{d}_i$ by $\mathbf{d}_i'=\sum_j S_{ij}\mathbf{d}_j$, where the matrix S is given by

$$\frac{1}{2}\begin{bmatrix} 1 & 1 & 1 & 1 & 1 & 1 \\ 1 & 1 & 1 & -1 & -1 & 1 \\ 1 & 1 & 1 & 1 & -1 & -1 \\ 1 & -1 & 1 & 1 & 1 & -1 \\ 1 & -1 & -1 & 1 & 1 & 1 \\ 1 & 1 & -1 & -1 & 1 & 1 \end{bmatrix}. \qquad (5)$$

The matrix also transforms the indices h_i by the same rule $h_i'=\sum_j S_{ij}h_j$ and the extinction rules are left invariant under the change of the unit vectors. Since $\det\underline{S}=1$, $\mathbf{d}_i'$ span the same lattice as $\mathbf{d}_i$ together with the corresponding centering translation vectors. These give different settings for the same lattice and indicate that there are an infinite number of settings. For the primitive lattice, $\mathbf{d}_i'$ related with $\mathbf{d}_i$ by $S^3=2S+1$ (instead of S) span the same lattice. [Note that $\frac{1}{2}(1,1,1,1,1,1)$, etc., are not the lattice points in this case.] The matrix S inflates the external component by the factor of τ and deflates the

internal component by the same factor.

From the above considerations, we can conclude that the lattice constant of the centered lattice has an ambiguity of the factor of τ and for the primitive one, the factor is τ^3. In the present case, there are odd-parity reflections, so that the lattice is primitive. The ambiguity of the lattice constant means that there are an infinite number of descriptions for the same structure as shown below. Hereafter we consider only the primitive lattice.

III. ICOSAHEDRAL CRYSTAL IN THE SIX-DIMENSIONAL SPACE

We discuss the basic ideas necessary to construct a model with the local atomic arrangement similar to that of the α phase in order.

A. The 3D Penrose lattice

As shown first by Duneau and Katz,[4] the diffraction patterns of the 3D Penrose lattice are similar to those of the Al-Mn alloy. This suggests that the *i* phase is related to the 3D Penrose lattice. The 3D Penrose lattice is given by the section of the 6D crystal in which the atom is located at the origin of the 6D unit cell. The atom is continuous within the domain defined by the set of $\mathbf{r}=\sum_j \lambda_j \mathbf{d}_j^i$ $(-\frac{1}{2}<\lambda_j\le\frac{1}{2})$, where the superscript i means the internal component. The domain is the rhombic triacontahedron with the edge length equal to ca [Fig. 1(a)]. The occupation function is 1 within the domain and 0 otherwise. The domain is referred to as the occupation domain hereafter. The structure factor is given by the Fourier transformation of this crystal. This derivation of the 3D Penrose lattice is equivalent to the projection method developed by several people.[4,5,12] In this case a agrees with the edge length of two unit rhombohedra in the 3D Penrose lattice (Fig. 2). There are, however, an infinite number of derivations which are within the related ambiguity of the lattice constant a in Eq. (3) of the factor of τ^3, and for every one of these lattice constants, we can derive the same 3D Penrose lattice from an atom with an appropriate occupation function placed at each 6D lattice point as shown below. The same lattice is also spanned by $\mathbf{d}_i'=\sum_j (S^3)_{ij}\mathbf{d}_j$, as shown in the previous section, but their external components inflate and internal components deflate by the factor of τ^3. The new unit vectors $\mathbf{d}_i'$ are expressed as $\mathbf{d}_1'=a'(\mathbf{a}_1,c'\mathbf{a}_1)$, $\mathbf{d}_j'=a'(\mathbf{a}_j,-c'\mathbf{a}_{2j})$ $(j=2,\ldots,6)$ with $a'=\tau^3 a$, $c'=\tau^{-6}c$. It is clear that if we use the same occupation function in this lattice, we have the same 3D section as the original setting described above. Then the rhombic triacontahedral occupation domain is expressed in terms of $\mathbf{d}_i'$ as the set of $\mathbf{r}=\sum_j \lambda_j \mathbf{d}_j'$ $(-\tau^3/2<\lambda_j<\tau^3/2)$. Thus we have an infinite number of descriptions for the same structure. The situation is analogous to that in the monoclinic and triclinic lattices in the 3D space. For these cases, we can select a reduced cell in which the off-diagonal terms in the metric tensor is minimum in the absolute value. For the present case, the reduced cell cannot be defined in such a way because the scale factor c in the internal space does not have a physical meaning and this makes it possible to reduce the off-diagonal elements to an arbitrarily small value for any setting. (This means that we can take the hypercubic lattice, but it should be noted that the symmetry of the structure is still icosahedral because the atom is continuous in the internal space and as a result the external space is not equivalent to the internal space.) Accordingly, the selection of the unit vectors is left ambiguous and the lattice constant cannot be determined uniquely. The above consideration concludes that the two settings employed by Elser[5] and Bancel *et al.*[25] are equivalent. For convenience we employ the former setting. Then $a=4.6$ Å for the Al-Mn alloy.

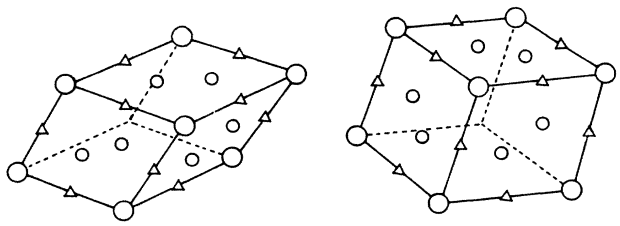

FIG. 2. Possible atomic sites in the unit rhombohedra of the 3D Penrose lattice. Mn atoms take the vertex positions (large circle) while Al(α) atoms are at the edge center (triangle). Al(β) and linking atoms occupy the vertex and one of two face-diagonal positions. The face-diagonal positions divide the longer face diagonal into the ratio of $\tau^{-2}:\tau^{-3}:\tau^{-2}$ (small circle).

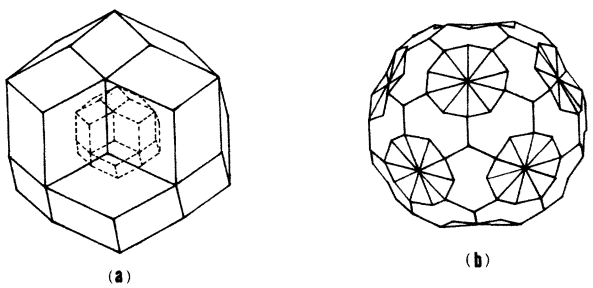

FIG. 1. (a) The occupation domain of the 3D Penrose lattice (solid line) and that of the icosahedral site (dotted line). (b) The shape of the occupation domain of the vacant site. This is obtained from the occupation domain of the icosahedral site by truncating a tip on the fivefold axis (Ref. 27).

B. The Mackay icosahedron

When we place an atom at each vertex derived by the method mentioned above (vertex model), the model shows diffraction patterns similar to those of Al-Mn alloy. From this fact, we first considered models with simple decorations which give a reasonable chemical composition and density. The models, however, failed to explain the diffraction pattern except for the disorder model in which Al atoms occupy some sites with the probability less than $\frac{1}{2}$. (See Sec. VI A.) On the other hand, Elser *et al.* point out that the cubic α phase[26] shows the diffraction intensity analogous to that of the quasicrystal

besides its symmetry. This consists of bcc packing of the icosahedral clusters including 42 Al, 2 Mn, and linking atoms connecting the icosahedral clusters. The center of this icosahedron (Mackay icosahedron) is vacant. We consider the quasicrystal consisting of the Mackay icosahedra. The essential difference in between the i phase and α phase is the symmetry. In order to consider the symmetry, we remark upon a different characteristic of the 3D Penrose lattice and the α phase. The skeleton of both structures consists of acute and obtuse golden rhombohedra with edge length of about 4.6 Å. All of their rhombic faces are the golden rhombus with two diagonals having the ratio of the golden number $\tau=(1+\sqrt{5})/2$. Both phases have the sites surrounded by 12 icosahedrally coordinated vertices (hereafter referred to as the icosahedral sites). The site is vacant, and the 12 neighboring vertices are occupied by Mn in the α phase. These Mn and the 42 Al construct the Mackay icosahedron around the icosahedral site. The distribution of the icosahedral sites in the 3D Penrose lattice is known.[27] This is obtained from the small triacontahedral occupation domain analogous to that mentioned in Sec. III A but with an edge length of $\tau^{-2}ca$ [dashed triacontahedron in Fig. 1(a)]. If we can construct the Mackay icosahedron at all the icosahedral sites in the 3D Penrose lattice, we will have the icosahedral structure with the local atomic arrangement similar to that of the α phase. Such a model is given by taking the four steps shown below.

First we consider the distribution of the centers of the Mackay icosahedra. In the α phase, the nearest-neighbor distance of the Mackay icosahedron is $2.384a$ while the $2\tau^{-5}$ sector of icosahedral sites in the 3D Penrose lattice has a shorter nearest-neighbor distance of a. These sites correspond to the places where two Mackay icosahedra penetrate within each other. Such sites are not present in the α phase. In order to avoid such a short distance, the small triacontahedral occupation domain mentioned above has to be truncated at the tip along the fivefold axis. The truncated portion is τ^{-5} of the triacontahedron. The shape of this occupation domain (hereafter referred to as the occupation domain of vacant sites) is illustrated in Fig. 1(b).

Around the vacant sites obtained this way, 12 Mn atoms are situated forming the regular icosahedron. When the origin is taken at the vacant site, such Mn sites are obtained from the occupation domains with the same shape and size as the occupation domain of vacant sites. These are located at $\mathbf{d}_1^e$ and positions related with this by the symmetry operations of the icosahedral $m\bar{3}\bar{5}$. This is because $\mathbf{d}_1^e$ has no internal component. This site is invariant under a fivefold axis and a mirror plane including the axis: The site symmetry is $5m$. Therefore all (120) the symmetry operations in $m\bar{3}\bar{5}$ create 12 equivalent positions. Their internal components are zero and therefore all the occupation domains for these positions are overlapped in the internal space. This domain is transformed onto itself by all the symmetry operators because it has icosahedral symmetry as shown in Fig. 1(b).

Similarly, 12 Al atoms at the edge center joining the vacant site and the neighboring 12 Mn sites are obtained from the same occupation domain at $\pm\mathbf{d}_j^e/2$ ($j=1,2,\ldots,6$), which are related with $\mathbf{d}_1^e/2$ by the symmetry operations. This is referred to as an Al(α) site. Their site symmetry is also $5m$. It is clear that if the vacant sites appear in the external space, then these 12 Mn and 12 Al sites also appear because their occupation domains spread in the internal space over the same range as that of the vacant sites.

The other 30 Al atoms [Al(β)] should be located on $(\mathbf{d}_1-\mathbf{d}_2)^e$ and sites derived from this by the symmetry operations. When the same occupation domains are placed at $(\mathbf{d}_1-\mathbf{d}_2)^e$ and equivalent positions, there exist 30 atoms around each lattice point which have the same internal position. These sites are invariant under the twofold axis and the mirror planes including the axis, and their site symmetry is $2mm$. The position in the external space is on the longer face diagonal of each rhombus of the acute and obtuse rhombohedra which divides its length into τ^{-2}:τ^{-1}. (See Fig. 2.) Since their occupation domain agrees with that of the vacant sites, if a vacant site appears in the external space, 30 Al atoms appear around it.

This quasicrystal consisting of only Mackay icosahedra has the icosahedral point group $m\bar{3}\bar{5}$, the order of which is 120. The superspace group is symmorphic and the lattice is primitive: this has no centering translation. The superspace group is $Pm\bar{3}\bar{5}$. The model gives a density of 2.68 g/cm^3 which is much smaller than that (3.52 g/cm^3) of an icosahedral Al_4Mn structure.[28] The chemical composition is about $Al_{3.3}Mn$ (23.2 at. % Mn). The Mn percentage is about the same as that of the stoichiometric composition (22 at. % Mn).[28] This implies that Mn linking atoms exist together with Al linking atoms, as in the α-phase.

C. Linking atoms

We consider the occupation domain to have the same shape as the occupation domain of the vacant sites, but enlarged by a factor (in a linear dimension) of τ^3. When this occupation domain is situated at each lattice point of the 6D lattice, we have a 3D Penrose pattern decorated with an additional vertex on the face diagonal of most golden rhombuses and on the body diagonal of some (few) acute rhombohedra in the usual 3D Penrose pattern. The relation between the decorated 3D Penrose and the usual 3D Penrose pattern is the same as that between the icosahedral vertex and the 3D Penrose pattern inflated with a factor of τ^3. The latter is examined by Henley and therefore the nature of the decorated Penrose pattern is known.[27] In particular, it is noted that its nearest-neighbor distance is $0.563a$ (2.59 Å for $a=4.6$ Å). The crystal chemical consideration allows us to place Al or Mn atoms for all the vertices. However, the center of the Mackay icosahedron should be vacant. This is achieved by considering the occupation domain with the vacant core at the center, the shape of which agrees with that of the occupation domain of the vacant sites. Furthermore, since this occupation domain includes the 12 occupation domains for Mn sites and 30 occupation domains for Al(β) sites shown in Fig. 3 (see Appendix), we have to re-

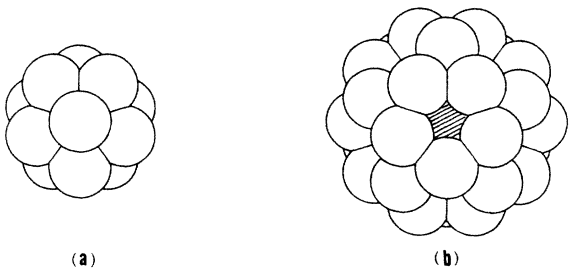

FIG. 3. (a) A part of the occupation domain cluster, which consists of the domains for 12 Mn. This is located at the center of the cluster shown in (b). Each domain has the shape shown in Fig. 1(b) but is denoted by a sphere with the same volume for simplicity. Each domain is in contact with the other sharing a plane normal to the twofold axis of the domain. The figure shows the view along the fivefold axis of the cluster. (b) The occupation domain cluster around each lattice point. The domains for 12 Mn and 30 Al(β) construct a cluster with the icosahedral symmetry. These domains are in contact with each other sharing ten planes of Fig. 1(b) around the fivefold axis or the plane normal to the twofold axis. Only 25 domains for Al(β) and one for Mn (shaded part) are visible.

move these occupation domains to get the occupation domain of the linking atom. Thus for the linking atom, the occupation domain has a complex shape including 43 vacant cores. When we place atoms for all the sites derived from such an occupation domain, we have an unacceptably large density. From this reason, we assume that the linking atom takes these vertices with the occupation probability of $\frac{1}{2}$. In order to get the reasonable chemical composition, it is assumed that the chemical composition of the linking atom is the same as that of the Mackay icosahedron and Mn and Al are randomly distributed at these sites. This model gives a reasonable density of 3.55 g/cm^3 and the chemical composition of $Al_{3.3}Mn$ (23.2 at. % Mn).

IV. STRUCTURE FACTOR

The structure factor of the model is given by the Fourier transformation of the 6D crystal. Although we can derive the analytical structure-factor formula for such a complex structure model,[29] we employ an approximation in which the shape of each occupation domain in the internal space is replaced with spheres having the same volume. This is a good approximation because each occupation domain is nearly spherical. The validity of the approximation for the strong reflection is confirmed by comparing the structure factor of the 3D Penrose pattern in this approximation with the exact one.[29] We employ the isotropic overall temperature factor for simplicity. The effect of the phason condensation is taken into account by an additional factor $\exp[-B'(\mathbf{q}^i)^2/4]$.[2] The structure factor in this approximation is given by

$$F(q)=\exp[-B(\mathbf{q}^e)^2/4-B'(\mathbf{q}^i)^2/4]\sum_{\mu}\left[f^{\mu}(\mathbf{q}^e)p^{\mu}m^{\mu}\sum_{(R\mid\tau)}\exp\left[2\pi i\sum_j h_j(R\mathbf{x}^{\mu})_j+h_j\tau_j\right]F_0^{\mu}(R^{-1}\mathbf{q}^i)\right], \tag{6}$$

where B is the isotropic overall temperature factor, $f^{\mu}(\mathbf{q}^e)$ represents the atomic scattering factor of μth atom in the 6D unit cell, p^{μ} the occupation probability, m^{μ} the multiplicity, R the rotation operator in the icosahedral group, and $(R\mathbf{x}^{\mu})_i$ and τ_i are the $\mathbf{d}_i$ components of the positional vector $R\mathbf{x}^{\mu}$ and translation vector τ accompanied by the rotation operator. The superspace group is symmorphic as mentioned above, so that $\tau_i=0$ (mod1) for all the rotation operators. $F_0^{\mu}(\mathbf{q}^i)$ stands for the Fourier integral of the function which takes one within the sphere of the radius r^{μ} and zero otherwise. This is written as

$$F_0^{\mu}(\mathbf{q}^i)=4\pi(r^{\mu})^3(\sin s^{\mu}-s^{\mu}\cos s^{\mu})/(s^{\mu})^3 \tag{7}$$

with $s^{\mu}=2\pi q^i r^{\mu}$. In Eq. (6), the summation with respect to μ is taken over all the independent atoms. In the present case there are four independent atom sites mentioned in the previous section. Of these, the linking-atom site has a complex occupation domain with vacant core. To calculate the structure factor for this site, we use the linearity of the Fourier transformation. The structure factor is obtained, from the structure factor of the large sphere, by subtracting the contribution of the vacant cores. The summation of $(R\mid\tau)$ is over all (120) symmetry operators of the icosahedral group. The matrix representation of the rotation operator R is defined by $R\mathbf{d}_i^*=\sum_j R_{ij}^{-1}\mathbf{d}_j^*$. Then $(R\mathbf{x})^i$ is expressed as $\sum_j R_{ij}x_j$. The matrix representation of the icosahedral group generators has been given by Janssen.[8] As is clear from Eq. (7), the diffraction intensity strongly depends on the value of q^i. The dependence of $(q^i)^{-3}$ means that only reflections with small q^i give strong diffraction intensities, though the phase factor in (6) may reduce the intensity of several reflections. It should be noted that (7) is applicable to all quasicrystals with spherical occupation domains. In more general cases in which the occupation domain is not spherical, $F_0^{\mu}(\mathbf{q}^i)$ in (7) will depend on the direction of $\mathbf{q}^i$ in addition to its length.

V. DIFFRACTION PATTERNS

The values of x_i^{μ}, r^{μ}, p^{μ}, and m^{μ} for the independent atoms in the present model are listed in Table I and the calculated electron diffraction patterns from this model are shown in Fig. 4 together with the observed patterns for Al_4Mn. (In Table I, the positions of each atom $(\mathbf{d}_1^e,\mathbf{d}_1^e/2,\mathbf{d}_1^e-\mathbf{d}_2^e)$ are expressed in terms of the 6D coordinates x_j. The coordinates are obtained by using the relations of $\mathbf{d}_1^e=[\mathbf{d}_1+(\mathbf{d}_2+\mathbf{d}_3+\mathbf{d}_4+\mathbf{d}_5+\mathbf{d}_6)/\sqrt{5}]/2$, etc.) The figure shows that the electron diffraction patterns

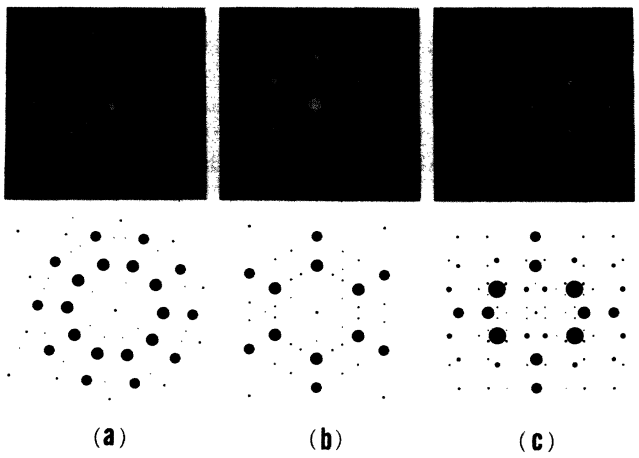

FIG. 4. The observed (top) and calculated (bottom) electron diffraction patterns of the icosahedral phase of an Al-Mn alloy. (a) Fivefold axis. (b) Threefold axis. (c) Twofold axis. The structure factors within the range of $-5 \leq h_i \leq 5$ $(i=1,\ldots,6)$ are calculated and reflections above a given threshold are plotted. The radii of the circles are proportional to the structure factors.

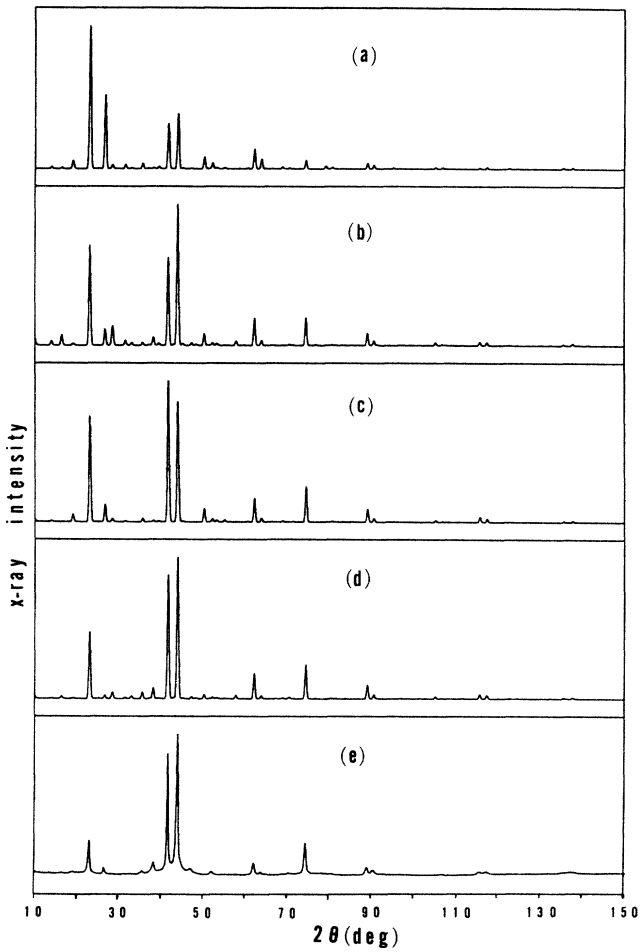

FIG. 5. The (a)–(d) calculated and (e) observed x-ray powder diffraction patterns. (a) Vertex model. (b) Guyot-Audier model. (c) Modified Hirage-Hirabayashi model. (d) The model proposed in this paper. (e) $Al_{76}Si_6Mn_{20}$. The half width at half maximum is assumed to be 0.25° in the calculation and the single Gaussian line shape is employed.

along fivefold, threefold, and twofold axes are well explained by the model. The x-ray powder pattern is illustrated in Fig. 5(d). This simulates an experimental result in Fig. 5(e) taken from $Al_{74}Si_6Mn_{20}$ with Cu $K\alpha$ radiation monochromatized by graphite monochromater. The parameters in this analysis are B and B', which are adjusted so as to explain the diffraction intensity. The experimental results require a large temperature factor, $B=4$ Å^2, and $B'=4(ca)^2$. These suggest that Mn and Al atoms are statistically distributed within the range of about ± 0.23 Å around their regular positions and the large structural fluctuation due to the phason, exists.[2,3]

The neutron powder-diffraction pattern gives new information. Dubois *et al.*[30] carried out the neutron diffraction experiment for $Al_{85}Si_1Mn_{14}$ and $Al_{85}Si_1(Mn_{0.72}Fe_{0.28})_{14}$. The former shows a diffraction pattern different from the x-ray pattern because Al and Mn have a scattering factor with opposite sign. In the latter, the same site is occupied randomly by Mn and Fe and the ratio of Mn and Fe are selected so as to cancel the scattering factors with each other. (Mn and Fe have neutron scattering factors with opposite sign.) This provides information on the Al site. Respecting that the powder-diffraction pattern gives only limited information

TABLE I. The atom coordinates x_i $(i=1,\ldots,6)$, the radius of the spherical occupation domain r, ca, the occupation probability p and the multiplicity m for each atomic site. Al/Mn(2)–Al/Mn(4) with negative p must be taken into account for the vacant cores in the occupation domain of the linking atom.

Atom	x_1	x_2	x_3	x_4	x_5	x_6	r	p	m
Mn	0.5	0.2236	0.2236	0.2236	0.2236	0.2236	0.5315	1	$\frac{1}{10}$
Al(α)	0.25	0.1118	0.1118	0.1118	0.1118	0.1118	0.5315	1	$\frac{1}{10}$
Al(β)	0.2764	−0.2764	0.0	0.4472	0.4472	0.0	0.5315	1	$\frac{1}{4}$
Linking atom									
Al/Mn(1)	0.0	0.0	0.0	0.0	0.0	0.0	2.2511	0.5	$\frac{1}{120}$
Al/Mn(2)	0.0	0.0	0.0	0.0	0.0	0.0	0.5315	−0.5	$\frac{1}{120}$
Al/Mn(3)	0.5	0.2236	0.2236	0.2236	0.2236	0.2236	0.5315	−0.5	$\frac{1}{10}$
Al/Mn(4)	0.2764	−0.2764	0.0	0.4472	0.4472	0.0	0.5315	−0.5	$\frac{1}{4}$

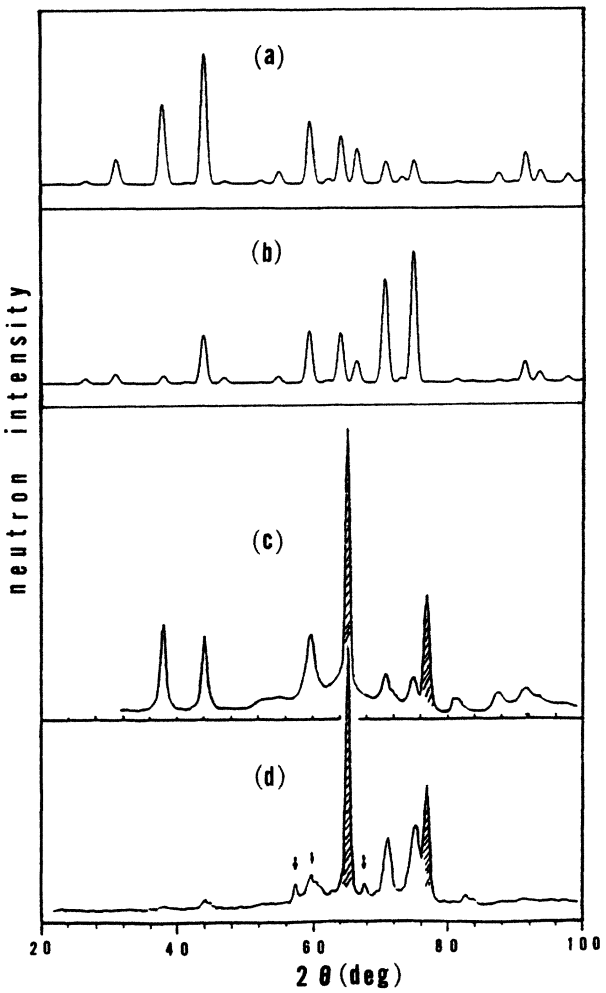

FIG. 6. The calculated [(a) and (b)] and observed [(c) and (d)] neutron powder-diffraction patterns (Ref. 30). (a) The total contribution of the present model. (b) Al contribution. (c) $Al_{85}Si_1Mn_{14}$. (d) $Al_{85}Si_1(Mn_{0.72}Fe_{0.28})_{14}$. The assumed half width at half maximum is 0.5°. The hatched lines in (c) and (d) are attributed to the cubic Al.

compared with the single-crystal experiment, we calculate the neutron powder pattern for these cases based on the model mentioned above. The results are shown in Fig. 6 together with the experimental results. In the figure, the hatched lines are attributed to the fcc Al. Since the chemical composition of the samples used is different from that of the present model, the detailed comparison is meaningless, but it is noted that except for the hatched lines, the calculated pattern can explain well the characteristic feature of the experimental data. In particular, Fig. 6(b) shows that the model describes well the distribution of Al.

VI. DISCUSSION AND CONCLUSION

A. Comparison with the other models

To compare the present model to other models proposed so far, we calculated the powder x-ray diffraction patterns for several models. The models considered here are (1) the vertex model, (2) the Guyot-Audier model,[20] and (3) a modified Hiraga-Hirabayashi model. We use the common temperature factors B and B' for all the models for comparison. The structure factor of the vertex model is known.[31] We placed Mn atoms at all the vertices. The Guyot-Audier model seems to agree with the model consisting only of Mn, Al(α), and Al(β) sites as described in Sec. III. The last model is obtained from the Hiraga-Hirabayashi (HH) model.[19] In the HH model, Mn atoms are placed in the vertex position of the 3D Penrose lattice and Al are on the two positions of the longer face diagonal of each golden rhombus which divide the diagonal into $\tau^{-2}:\tau^{-3}:\tau^{-2}$, with an occupation probability of $\frac{1}{2}$ (Fig. 2). Although this model gives better diffraction patterns than the other two models, a slight modification shows much better diffraction patterns. The modified Hiraga-Hirabayashi model places Al at the face diagonal positions mentioned above, with an occupation probability of 0.4, and at the edge-center position with an occupation probability of 0.2. Since the Al sites have occupation domains far from the sphere (the rhombic icosahedron and rhombic dodecahedron), we use the analytical expression for the structure factor. The structure-factor formula (6) is applicable, but the expression of $F_0^{\mu}(\mathbf{q}^i)$ is different from (7). The explicit expression for $F_0^{\mu}(\mathbf{q}^i)$ is referred to in Ref. 29. The former two are unrealistic models in the sense that the chemical composition or the density does not agree with the experimental value. On the other hand, the third model gives reasonable chemical composition and density (25 at. Mn, 3.57 g/cm^2). Mn atoms are completely ordered while Al atoms are completely disordered. The former two models qualitatively explain the diffraction pattern [Figs. 5(a) and 5(b)] but the agreement with the experiment is not enough. The last model gives a better result [Fig. 5(c)]. In order to check the validity of this model we calculated the neutron diffraction patterns, but the model failed to explain these patterns. In particular, the Al contribution of this model shows two strong lines around $2\theta=40°$, in contrast to the experimental result of $Al_{85}Si_1(Mn_{0.72}Fe_{0.28})_{14}$ [see Fig. 6(d)].

B. Meaning of the large temperature factor

The large temperature factor may suggest another possibility, that in the real structure each atom may displace around the ideal position considered above. This is taken into account by using the displacement field $\mathbf{u}^e(\mathbf{r}^i)$ which is parallel to the external space and dependent on the internal coordinates. In fact, the displacement from the ideal position is observed in the α phase. The average displacement of 0.23 Å is a reasonable value in comparison with that of the α phase. The refinement of the model is the subject of further study.

C. Conclusion

The present analysis shows that the i-Al-Mn quasicrystal consists of the Mackay icosahedra and the linking-Al or Mn joining them. The Mackay icosahedra

are situated on the icosahedral sites of the 3D Penrose pattern. The section method is efficient in describing such a complex model in the superspace and in calculating the structure factor.

ACKNOWLEDGMENTS

The authors thank Professor T. Masumoto, Tohoku University for supplying an i-$Al_{74}Si_6Mn_{20}$ sample. One of the authors (A.Y.) also thanks Professor S. Takeuchi, Dr. K. Kimura, the Institute of Solid State Physics, the University of Tokyo, Professor T. Ogawa, Tsukuba University, and Dr. F. Izumi, National Institute for Research in Organic Materials (NIRIM), for valuable discussions, and Mr. T. Wada, NIRIM, for technical support on the x-ray diffraction experiment.

APPENDIX

The occupation domains of Mn and Al(β) form a cluster with the icosahedral symmetry in the internal space near each lattice point. The occupation domain of Mn at $-\mathbf{d}_1+\mathbf{d}_1^e$ is located at the internal space which passes through the origin. From $\mathbf{d}_1=\mathbf{d}_1^e+\mathbf{d}_1^i$, we have the occupation domain belonging to the lattice point $-\mathbf{d}_1$ at $-\mathbf{d}_1^i$. The 12 equivalent positions obtained from $-\mathbf{d}_1^i$ are situated at the tips of the regular icosahedron forming the icosahedral cluster [Fig. 3(a)]. Similarly, the occupation domain of Al(β) at $-(\mathbf{d}_1-\mathbf{d}_2)+(\mathbf{d}_1-\mathbf{d}_2)^e=-(\mathbf{d}_1-\mathbf{d}_2)^i$ and the domains equivalent to it construct a cluster consisting of 30 domains in the same internal space (through the origin) [Fig. 3(b)]. Note that $|\mathbf{d}_1^i|=ca$ and $|(\mathbf{d}_1-\mathbf{d}_2)^i|=1.7016ca$. The average radius of these domains is $0.5315ca$ while that of the domain for the linking atoms, considered in the text, is $2.251ca$. (See Table I.) This shows that the latter includes the 12 domains for Mn and 30 domains for Al(β). It should be noted that the domains at $-\mathbf{d}_1^i$ and $-(\mathbf{d}_1-\mathbf{d}_2)^i$ or their equivalent pair of domains contact with each other sharing the ten planes of Fig. 1(b) around the fivefold axis. The distance of the centers is ca while the average radius of the domains is $0.5315ca$. Therefore these two may be partly overlapped. There exists, however, no overlapped part in the real domains because of their shape [Fig. 1(b)]. Similar consideration shows that the domain at $-\mathbf{d}_1^i$ and $-\mathbf{d}_2^i$ or $-(\mathbf{d}_1-\mathbf{d}_2)^i$ and $-(\mathbf{d}_1-\mathbf{d}_3)^i$ or their equivalent domains also contact sharing the plane normal to the twofold axis. As a result, all (42) the domains are connected to form a multiply connected cluster. This cluster is not overlapped with the occupation domain of the vacant sites which is located at the center of the cluster due to the shape of the domains. (Note that the domains for 12 Mn are also ca apart from the origin.)

[1]D. Shechtman, I. Blech, D. Gratias, and J. W. Cahn, Phys. Rev. Lett. **53**, 1951 (1984).
[2]P. A. Kalugin, A. Yu. Kitayev, and L. S. Levitov, J. Phys. (Paris) Lett. **46**, L601 (1985).
[3]P. A. Kalugin, A. Yu. Kitaev, and L. S. Levitov, Pis'ma Zh. Eksp. Teor. Fiz. **41**, 119 (1985) [JETP Lett. **41**, 145 (1985)].
[4]M. Duneau and A. Katz, Phys. Rev. Lett. **54**, 2688 (1985).
[5]V. Elser, Phys. Rev. B **32**, 4892 (1985).
[6]R. K. P. Zia and W. J. Dallas, J. Phys. A **18**, L341 (1985).
[7]V. Elser and C. L. Henley, Phys. Rev. Lett. **55**, 2883 (1985).
[8]T. Janssen, Acta Crystallogr. Sect. A **4**, 261 (1986).
[9]T. Ogawa, J. Phys. Soc. Jpn. **54**, 3205 (1985).
[10]R. Penrose, Math. Intell. **2**, 32 (1979).
[11]A. L. Mackay, Kristallografiya **26**, 910 (1981) [Sov. Phys.—Crystallogr. **26**, 517 (1981)]; A. L. Mackay, Physica A **114**, 609 (1982).
[12]P. Kramer and R. Neri, Acta Crystallogr. Sect. A **40**, 580 (1984).
[13]J. E. S. Socolar, P. J. Steinhardt, and D. Levine, Phys. Rev. B **32**, 5547 (1985).
[14]D. Levin and P. J. Steinhardt, Phys. Rev. Lett. **53**, 2477 (1985).
[15]L. A. Bursill and P. J. Lin, Nature (London) **316**, 50 (1985).
[16]K. Hiraga, M. Hirabayashi, A. Inoue, and T. Masumoto, J. Phys. Soc. Jpn. **54**, 4077 (1985).
[17]K. N. Ishihara and P. H. Shingu, J. Phys. Soc. Jpn. **55**, 1795 (1986).
[18]S. Takeuchi and K. Kimura, in Proceedings of the First International Symposium for Science of Form, University of Tsukuba, 1985 (unpublished).
[19]K. Hiraga and M. Hirabayashi, in Proceedings of the First International Symposium for Science of Form, University of Tsukuba, 1985 (unpublished).
[20]P. Guyot and M. Audier, Philos. Mag. B **52**, L15 (1985); M. Audier and P. Guyot, Philos. Mag. B **53**, L43 (1986).
[21]Per Bak, Phys. Rev. Lett. **56**, 861 (1986).
[22]P. M. de Wolff, Acta Crystallogr. A **30**, 777 (1974).
[23]A. Janner and T. Janssen, Physica A **99**, 47 (1979).
[24]A. Yamamoto, Acta Crsytallogr. B **38**, 1451 (1982).
[25]P. A. Bancel, P. A. Heiney, P. W. Stephens, A. I. Goldman, and P. M. Horn, Phys. Rev. Lett. **54**, 2422 (1985).
[26]M. A. Taylor, Acta Metall. **8**, 256 (1960).
[27]C. L. Henley, Phys. Rev. B **34**, 797 (1986).
[28]K. Kimura, T. Hashimoto, K. Suzuki, K. Nagayama, H. Ino, and S. Takeuchi, J. Phys. Soc. Jpn. **54**, 3217 (1985).
[29]A. Yamamoto (unpublished).
[30]J. M. Dubois, C. Janot, and J. Pannetier, Phys. Lett. **115A**, 117 (1986).
[31]V. Elser, Acta Crystallogr. Sect. A **42**, 36 (1986).

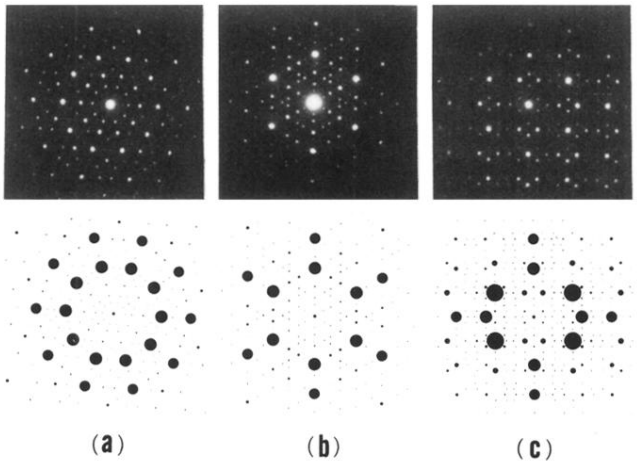

FIG. 4. The observed (top) and calculated (bottom) electron diffraction patterns of the icosahedral phase of an Al-Mn alloy. (a) Fivefold axis. (b) Threefold axis. (c) Twofold axis. The structure factors within the range of $-5 \leq h_i \leq 5$ $(i = 1, \ldots, 6)$ are calculated and reflections above a given threshold are plotted. The radii of the circles are proportional to the structure factors.